

1 **Accounting for diverse evolutionary forces reveals the mosaic nature of selection on genomic**
2 **regions associated with human preterm birth**

3 **Authors:** Abigail L. LaBella[†], Abin Abraham[†], Yakov Pichkar, Sarah L. Fong, Ge Zhang, Louis J.
4 Muglia, Patrick Abbot, Antonis Rokas*, & John A. Capra*

5 [†]Co-first Authors, *Co-corresponding Authors

6
7 *Abin Abraham:* Vanderbilt Genetics Institute, Vanderbilt University, Nashville, TN 37235, USA ,
8 Vanderbilt University Medical Center, Vanderbilt University, Nashville, TN 37232, USA
9 ORCID: 0000-0002-9951-2879

10 *Abigail L. LaBella:* Department of Biological Sciences, Vanderbilt University, Nashville, TN 37235, USA
11 ORCID: 0000-0003-0068-6703

12 *Yakov Pichkar:* Department of Biological Sciences, Vanderbilt University, Nashville, TN 37235, USA
13 ORCID: 0000-0001-9231-2180

14 *Sarah L. Fong:* Vanderbilt Genetics Institute, Vanderbilt University, Nashville, TN 37235, USA
15 ORCID: 0000-0003-0900-5505

16 *Ge Zhang:* Division of Human Genetics, Cincinnati Children's Hospital Medical Center, USA
17 The Center for Prevention of Preterm Birth, Perinatal Institute, Cincinnati Children's Hospital Medical Center, USA
18 March of Dimes Prematurity Research Center Ohio Collaborative, USA
19 Department of Pediatrics, University of Cincinnati College of Medicine, USA

20 *Louis J. Muglia:* Division of Human Genetics, Cincinnati Children's Hospital Medical Center, USA
21 The Center for Prevention of Preterm Birth, Perinatal Institute, Cincinnati Children's Hospital Medical Center, USA
22 March of Dimes Prematurity Research Center Ohio Collaborative, USA
23 Department of Pediatrics, University of Cincinnati College of Medicine, USA

24 *Patrick Abbot:* Department of Biological Sciences, Vanderbilt University, Nashville, TN 37235, USA

25 *John A. Capra*:* Department of Biological Sciences, Vanderbilt University, Nashville, TN, 37235, USA
26 Departments of Biomedical Informatics and Computer Science, Vanderbilt Genetics Institute, Center for Structural
27 Biology, Vanderbilt University, Nashville, TN, 37235, USA
28 Corresponding author: E-mail: tony.capra@vanderbilt.edu
29 ORCID: 0000-0001-9743-1795

30 *Antonis Rokas*:* Department of Biological Sciences, Vanderbilt University
31 Department of Biomedical Informatics, Vanderbilt University School of Medicine
32 Corresponding author: E-mail: antonis.rokas@vanderbilt.edu.
33 ORCID: 0000-0002-7248-6551

34

35 **ABSTRACT**

36 Human pregnancy requires the coordinated function of multiple tissues in both mother and fetus and has
37 evolved in concert with major human adaptations. As a result, pregnancy-associated phenotypes and
38 related disorders are genetically complex and have likely been sculpted by diverse evolutionary forces.
39 However, there is no framework to comprehensively evaluate how these traits evolved or to explore the
40 relationship of evolutionary signatures on trait-associated genetic variants to molecular function. Here we
41 develop an approach to test for signatures of diverse evolutionary forces, including multiple types of
42 selection, and apply it to genomic regions associated with spontaneous preterm birth (sPTB), a complex
43 disorder of global health concern. We find that sPTB-associated regions harbor diverse evolutionary
44 signatures including evolutionary sequence conservation (consistent with the action of negative selection),
45 excess population differentiation (local adaptation), accelerated evolution (positive selection), and
46 balanced polymorphism (balancing selection). Furthermore, these genomic regions show diverse
47 functional characteristics which enables us to use evolutionary and molecular lines of evidence to develop
48 hypotheses about how these genomic regions contribute to sPTB risk. In summary, we introduce an
49 approach for inferring the spectrum of evolutionary forces acting on genomic regions associated with
50 complex disorders. When applied to sPTB-associated genomic regions, this approach both improves our
51 understanding of the potential roles of these regions in pathology and illuminates the mosaic nature of
52 evolutionary forces acting on genomic regions associated with sPTB.

53

54 INTRODUCTION

55 Mammalian pregnancy requires the coordination of multiple maternal and fetal tissues^{1,2} and extensive
56 modulation of the maternal immune system so that the genetically distinct fetus is not immunologically
57 rejected³. Given this context, pregnancy-related phenotypes and disorders are likely to have experienced
58 diverse selective pressures. This is particularly likely on the human lineage where pregnancy has been
59 shaped by unique human adaptations such as bipedality and enlarged brain size⁴⁻⁸. One major disorder of
60 pregnancy is preterm birth (PTB), a complex multifactorial syndrome⁹ that affects 10% of pregnancies in
61 the United States and more than 15 million pregnancies worldwide each year^{10,11}. PTB leads to increased
62 infant mortality rates and significant short- and long-term morbidity¹¹⁻¹⁴. Risk for PTB varies
63 substantially with race, environment, comorbidities, and genetic factors¹⁵. PTB is broadly classified into
64 iatrogenic PTB, when it is associated with medical conditions such as preeclampsia (PE) or intrauterine
65 growth restriction (IUGR), and spontaneous PTB (sPTB), which occurs in the absence of preexisting
66 medical conditions or is initiated by preterm premature rupture of membranes¹⁶⁻¹⁹. The biological
67 pathways contributing to sPTB remain poorly understood⁹, but diverse lines of evidence suggest that
68 maternal genetic variation is an important contributor²⁰⁻²⁴.

69 The complexity of human pregnancy and association with unique human adaptations raise the hypothesis
70 that genetic variants associated with birth timing and sPTB have been shaped by diverse evolutionary
71 forces. Consistent with this hypothesis, several immune genes involved in pregnancy have signatures of
72 recent purifying selection²⁵ while others have signatures of balancing selection²⁵⁻²⁷. In addition, both birth
73 timing and sPTB risk vary across human populations²⁸, which suggests that genetic variants associated
74 with these traits may also exhibit population-specific differences. Variants at the progesterone receptor
75 locus associated with sPTB in the East Asian population show evidence of population-specific
76 differentiation driven by positive and balancing selection^{29,30}. Since progesterone has been extensively
77 investigated for sPTB prevention³¹, these evolutionary insights may have important clinical implications.
78 Although these studies have considerably advanced our understanding of how evolutionary forces have

79 sculpted specific genes involved in human birth timing, we lack a comprehensive examination of how
80 diverse evolutionary forces have influenced genomic regions involved in sPTB.

81 The recent availability of sPTB-associated genomic regions from large genome-wide association studies
82 (GWAS)³² coupled with advances in measuring evidence for diverse evolutionary forces—including
83 balancing selection³³, positive selection³⁴, and purifying selection³⁵ from human population genomic
84 variation data—present the opportunity to comprehensively survey how evolution has shaped sPTB-
85 associated genomic regions. To achieve this, we developed an approach that identifies evolutionary forces
86 that have acted on genomic regions associated with a complex trait and compares them to appropriately
87 matched control regions. Our approach innovates on current methods by evaluating the impact of multiple
88 different evolutionary forces on trait-associated genomic regions while accounting for genomic
89 architecture-based differences in the expected distribution for each of the evolutionary measures.

90 Application of our approach to 215 sPTB-associated genomic regions showed significant evidence for at
91 least one evolutionary force in 120 regions. Furthermore, we identified functional links to sPTB and other
92 pregnancy phenotypes for representative genomic regions exhibiting evidence for each evolutionary
93 force. These results suggest that a mosaic of evolutionary forces likely influenced human birth timing,
94 and that evolutionary analysis can assist in interpreting the role of specific genomic regions in disease
95 phenotypes.

96 **RESULTS & DISCUSSION**

97 **Evaluating the significance of evolutionary measures by accounting for genomic architecture**

98 In this study, we compute diverse evolutionary measures on sPTB-associated genomic regions to infer the
99 action of multiple evolutionary forces (Table 1). While various methods to detect signatures of
100 evolutionary forces exist, many of them lack approaches for determining statistically significant
101 observations or rely on the comparison to the distribution of the measure when applied genome-wide^{36,37}.
102 Furthermore, population level attributes, such as minor allele frequency (MAF) and linkage

103 disequilibrium (LD), influence the power to detect both evolutionary signatures³⁸⁻⁴⁰ and GWAS
 104 associations⁴¹. Thus, interpretation and comparison of different evolutionary measures is challenging,
 105 especially when the regions under study do not reflect the genome-wide background.

106 Here we develop an approach that derives a matched null distribution accounting for MAF and LD for
 107 each evolutionary measure and set of regions. We generate 5,000 control region sets that each match the
 108 trait-associated regions on these attributes (Methods). Then, to calculate an empirical p-value and z-score
 109 for each evolutionary measure and region of interest, we compare the median values of the evolutionary
 110 measure for variants in the sPTB-associated genomic region to the same number of variants in the
 111 corresponding matched control regions. This enables comparison across evolutionary measures and
 112 genomic regions (Figure 1A, Methods).

113

Table 1: Evolutionary measures computed on sPTB-associated genomic regions with the corresponding evolutionary signature used to infer the evolutionary force and the associated timescale. GERP: Genomic evolutionary rate profiling. iHS: integrated haplotype score. XP-EHH: cross-population extended haplotype homozygosity (EHH). iES: integrated site-specific EHH. TMRCA: time to most recent common ancestor derived from ARGweaver. Alignment block age was calculated using 100-way multiple sequence alignments to determine the oldest most recent common ancestor for each alignment block.

Measures	Evolutionary signature	Evolutionary force	Time scale
PhyloP	Substitution rate	Positive/negative selection	Across species
PhastCons	Sequence conservation	Negative selection	Across species
GERP			
LINSIGHT			Across species and human populations
F _{ST}	Population differentiation	Local adaptation	Human populations
iHS	Haplotype homozygosity	Positive selection	Human populations
XP-EHH			
iES			
Beta Score	Balanced polymorphisms	Balancing selection	Human populations
Allele Age (TMRCA)	Ancestral recombination graphs/Alignments	Evolutionary origin / Negative selection	Human populations
Alignment block age	Sequence conservation	Evolutionary origin / Negative selection	Across species

114

115 We used this approach to evaluate the evolutionary forces acting on genomic regions associated with
116 sPTB. First, we identified all variants nominally associated with sPTB ($p < 10E-4$) in the largest available
117 GWAS³² and grouped variants into regions based on high LD ($r^2 > 0.9$). It is likely that many of these
118 nominally associated variants affect sPTB risk, but did not reach genome-wide significance due to factors
119 limiting the statistical power of the GWAS³². Therefore, we assume that many of the variants with sPTB-
120 associations below this nominal threshold contribute to the genetic basis of this trait. This identified 215
121 independent sPTB-associated genomic regions, which we refer to by the lead variant (SNP or indel with
122 the lowest p-value in that region).

123 For each of the 215 sPTB-associated genomic regions, we generated control regions as described above.
124 The match quality per genomic region, defined as the fraction of sPTB variants with a matched variant
125 averaged across all control regions, is $\geq 99.6\%$ for all sPTB-associated genomic regions (Figure 1B). The
126 matched null distribution aggregated from the control regions varied substantially between sPTB-
127 associated genomic regions for each evolutionary measure and compared to the unmatched genome-wide
128 background distribution (Supplemental Figure 1). The F_{ST} measure between East Asians and Europeans
129 ($F_{ST-EurEas}$) illustrates this variation. Different sets of sPTB-associated genomic regions had statistically
130 significant ($p < 0.05$) median $F_{ST-EurEas}$ based on comparison to the unmatched genome-wide distribution
131 versus comparison to the matched null distribution (Figure 1C). Two regions (Figure 1C: red dots) were
132 statistically significant ($p < 0.05$) only when using our method due to the narrow shape of the matched null
133 distribution. In contrast, three other regions (Fig 1C: blue dots) were significant based on the genome-
134 wide distribution, but not using our method likely due to the genetic architecture of this region. Seven
135 regions (Fig 1C: black dots) were statistically significant using both methods. Similar results were
136 obtained across the other evolutionary measures (See Supplemental Figure 1 for break down by
137 evolutionary measure).

138 Our approach to test for signatures of different evolutionary forces has many advantages. Comparing
139 evolutionary measures against a null distribution that accounts for MAF and LD enables us to increase the

140 sensitivity with which we can infer the action of evolutionary forces on sets of genomic regions that differ
141 in their genome architectures. In addition, the lead SNPs assayed in a GWAS are often not the causal
142 variant, so by testing both the lead SNPs and those in LD when evaluating a genomic region for
143 evolutionary signatures, we are able to better represent the trait-associated evolutionary signatures
144 compared to other methods that evaluate only the lead variant⁴² or all variants, including those not
145 associated with the trait, in a genomic window⁴³ (Supplementary Table 1). Finally, our approach uses an
146 empirical framework that leverages the strengths of diverse existing evolutionary measures.

147 **Genomic regions associated with sPTB exhibit signatures of diverse modes of selection.**

148 To gain insight into the modes of selection that have acted on sPTB-associated genomic regions, we
149 focused on genomic regions with extreme evolutionary signatures by selecting the 120 sPTB-associated
150 regions with at least one extreme z-score ($z \geq \pm 1.5$) (Figure 2; Supplementary Tables 2 and 3) for
151 further analysis. Notably, each evolutionary measure had at least one genomic region with an extreme
152 observation ($p < 0.05$). Hierarchical clustering of the 120 regions revealed 12 clusters of regions with
153 similar evolutionary patterns. We manually combined the 12 clusters based on their dominant
154 evolutionary signatures into five major groups with the following general evolutionary patterns (Figure
155 2): conservation/negative selection (group A: clusters A1-4), excess population differentiation/local
156 adaptation (group B: clusters B1-2), positive selection (group C: cluster C1), long-term balanced
157 polymorphism/balancing selection (group D: clusters D1-2), and other diverse evolutionary signatures
158 (group E: clusters E1-4).

159 Previous literature on complex genetic traits⁴⁴⁻⁴⁶ and pregnancy disorders^{25,29,30,47,48} supports the finding
160 that multiple modes of selection have acted on sPTB-associated genomic regions. Unlike many of these
161 previous studies that tested only a single mode of selection, our approach tested multiple modes of
162 selection. Of the 215 genomic regions we tested, 9% had evidence of conservation, 5% had evidence of
163 excess population differentiation, 4% had evidence of accelerated evolution, 4% had evidence of long-
164 term balanced polymorphisms, and 34% had evidence of other combinations. From these data we infer

165 that negative selection, local adaptation, positive selection, and balancing selection have all acted on
166 genomic regions associated with sPTB, highlighting the mosaic nature of the evolutionary forces that
167 have shaped this trait. In addition to differences in evolutionary measures, variants in these groups also
168 exhibited differences in their functional effects, likelihood of influencing transcriptional regulation,
169 frequency distribution between populations, and effects on tissue-specific gene expression (Figure 3;
170 Supplementary Tables 4 and 5). We now describe each group and give examples of their members and
171 their potential connection to PTB and pregnancy.

172 **Group A: Sequence Conservation/Negative selection**

173 Group A contains 19 genomic regions and 47 total variants. Variants in this group had higher than
174 expected values for evolutionary measures of sequence conservation and alignment block age:
175 PhastCons100, PhyloP, allele age in TMRCA derived from ARGweaver, LINSIGHT and/or GERP
176 (Figure 2). The strong sequence conservation suggests that these genomic regions evolved under negative
177 selection. The average derived allele frequency of group A variants across populations is 0.15 (Figure
178 3C). The majority of variants are intronic (37/47: 79%) but a considerable fraction is intergenic (8/47:
179 17%; Figure 3B). One coding variant (rs17436878) results in a synonymous change in the gene *RGL1* and
180 another variant (rs6546891) is located in the 3' UTR of the Ten-Eleven Translocation Methylcytosine
181 Dioxygenase 3 (*TET3*) gene. Only one variant is predicted to affect regulatory binding (rs71483318,
182 RegulomeDB score=2), a finding consistent with the observation that most (41/47) variants in this group
183 are not known to be associated with expression changes (Figure 4D).

184 The sPTB-associated genomic region in the 3' UTR of the gene *TET3* has significant values for
185 LINSIGHT, GERP, and PhastCons100 (Figure 2). The G allele of rs6546891 is associated with a
186 nominally increased risk of sPTB in European ancestry individuals (OR: 1.13; adjusted p-value: 5.4×10^{-5})³². This risk allele (G) arose on the human lineage while the protective allele (A) is ancestral and is
187 present across the great apes (Figure 4A). The risk allele is the minor allele in all three populations
188 examined and has the lowest frequency in Europeans. Functionally, this variant is an eQTL for 76

190 gene/tissue pairs: most notably this variant is associated with the expression of the hypothetical protein
191 LOC730240 in the uterus, ovary, vagina, and brain as well as the expression of N-acetyltransferase 8
192 (*NAT8*) in the testis. The conservation detected at this locus suggests that disruptions in *NAT8* or *TET3*
193 are likely to be deleterious.

194 The genes *TET3* and *NAT8* are both linked to gestation and pregnancy outcomes. In mice, *TET3* affects
195 epigenetic reprogramming in oocytes and zygotes, is required for neonatal growth, and depletion of *TET3*
196 in female mice results in reduced fecundity^{49,50}. In humans, *TET3* expression was detected in the villus
197 cytotrophoblast cells in the first trimester as well as in maternal decidua of placentas⁵¹. Expression
198 profiling showed elevated *TET3* transcripts in preeclamptic placentas and in pregnancies ending with the
199 birth of a newborn that is small for gestational age (SGA)⁵². *TET3* is also hypothesized to play a role in
200 the link between preterm birth and the risk of neurodevelopmental disorders due to the gene's role in
201 epigenetic regulation⁵³. *NAT8*, which is involved in acetylation of histones, may also play a role in
202 epigenetic changes during pregnancy⁵⁴. The strong sequence conservation of the region containing
203 variant rs6546891 is consistent with previous findings that negative selection is the dominant mode of
204 selection for *TET3*⁵⁵. More broadly, these findings suggest that several sPTB-associated genomic regions
205 have experienced negative selection, consistent with previous studies^{42,56}.

206 **Group B: Population Differentiation/Population-specific Adaptation**

207 Group B (clusters B1 and B2) contained variants with a higher than expected differentiation (F_{ST})
208 between pairs of human populations (Figure 2). There were 10 sPTB-associated genomic regions in this
209 group, which contain 53 variants. Most variants in this group are intronic (38/53) while the rest are
210 intergenic (14/53) or located within 5000bp upstream of a gene (1/53) (Figure 3A). One variant
211 (rs3897712) may be involved in regulating transcription factor binding (Figure 3B), but is not a known
212 eQTL. For the remaining variants, the majority are an eQTL in at least one tissue (29/52; Figure 3D). The
213 derived allele frequency in cluster B1 is high in East Asian populations and very low in African and
214 European populations (Figure 3C). We found that 3 of the 10 lead variants have higher risk allele

215 frequencies in African compared to European or East Asian populations. This is noteworthy because the
216 rate of PTB is twice as high among black women compared to white women in the United States^{57,58}.
217 These three variants are associated with expression levels of the genes *SLC33A1*, *LOC645355*, and *GC*,
218 respectively.

219 The six variants within the sPTB-associated region near *GC*, Vitamin D Binding Protein, are of particular
220 interest. The lead variant is rs222016. The G allele of this lead variant (rs222016) has a higher frequency
221 in African populations, is the ancestral allele, and is associated with increased risk of sPTB (European
222 cohort, OR: 1.15; adjusted p-value 3.58×10^{-5} ; Figure 4B)³². This variant has also been associated with
223 vitamin D levels and several other disorders; for example, in individuals with ankylosing spondylitis the
224 G allele (risk for sPTB) is associated with increased risk of developing peripheral arthritis⁵⁹. This variant
225 is also associated with high baseline D3 levels in serum but is not associated with reduced risk of D3
226 insufficiency⁶⁰. There is also evidence that vitamin D levels prior to delivery are associated with sPTB,^{61–}
227 ⁶⁴ that levels of *GC* in cervico-vaginal fluid may help predict sPTB^{65,66}, and that vitamin D deficiency
228 may contribute to racial disparities in birth outcomes^{67,68}. Specifically, vitamin D deficiency may
229 contribute to potential risk for preeclampsia among Hispanic and African American women⁶⁹. The
230 population-specific differentiation associated with the variant rs222016 is consistent with the differential
231 evolution of the vitamin D system between populations—likely in response to different environments and
232 associated changes in skin pigmentation^{70,71}. Our results provide evolutionary context for the link between
233 vitamin D and pregnancy outcomes⁷² and suggest a role for variation in the gene *GC* in the ethnic
234 disparities in pregnancy outcomes.

235 **Group C: Accelerated substitution rates/Positive selection**

236 Variants in cluster C1 (group C) had lower than expected values of PhyloP. This group contains nine
237 sPTB-associated genomic regions and 232 total variants. The large number of linked variants is consistent
238 with the accumulation of polymorphisms in regions undergoing positive selection. The derived alleles in
239 this group show no obvious pattern in allele frequency between populations (Figure 3C). While most

240 variants in this group are intronic (218/232), there are missense variants in the genes Protein Tyrosine
241 Phosphatase Receptor Type F Polypeptide Interacting Protein Alpha 1 (*PPFIA1*) and Plakophilin 1
242 (*PKP1*; Figure 3A). Additionally, 16 variants in this group are likely to affect transcription factor binding
243 (regulomeDB score of 1 or 2; Figure 3B). Consistent with this finding, of the 216 variants tested in GTEx,
244 167 are associated with expression of at least one gene in one tissue (Figure 3C).

245 The lead variant associated with *PPFIA1* (rs1061328) is linked to an additional 156 variants, which are
246 associated with the expression of a total of 2,844 tissue/gene combinations. This variant (rs1061328) has
247 signatures of positive selection and is associated with the expression of genes involved in cell adhesion
248 and migration—critical processes in the development of the placenta. There are three alleles at this
249 locus—two (C and T) were examined in the sPTB GWAS, while the third (G allele) is rare. The risk
250 allele, C, is ancestral and is the major allele in the European and East Asian populations. The derived
251 protective allele (effect: 0.868, adjusted p-value 5.05×10^{-4})³² is the major allele in the African population.
252 The C→T polymorphism is synonymous (GAC→CAT) at an asparagine residue in the 14th of 28 exons
253 in the *PPFIA1* gene. A third derived allele (G) is present at very low frequency (<0.001%) and is a
254 missense mutation (asparagine→glutamic acid). There is one additional synonymous variant associated
255 with sPTB (rs17853270) in the 17th exon of *PPFIA1*. There are 156 variants linked to rs1601328, which
256 compose a large and complex haplotype spanning approximately 129 kb. This variant also affects
257 expression of two genes cortactin (*CTTN*) and *PPFIA1* in several tissues, including adipose, thyroid, and
258 tibial nerve (GTEx v7)⁷³.

259 Both *CTTN* and *PPFIA1* are involved in cell motility and cell adhesion. The PPFIA1 protein is a member
260 of the LAR protein-tyrosine phosphatase-interacting protein (liprin) family and is involved in cell
261 motility, extracellular matrix dynamics, and cell adhesion^{74–77}. Cell adhesion and migration are also
262 critical processes involved in placental development and implantation^{78,79} and other members of the liprin
263 family have been linked to maternal-fetal signaling during placental development^{80,81}. The *CTTN* protein
264 is an actin-binding protein involved in cell migration and invasion^{82–84}. *CTTN* was shown to be expressed

265 in the decidual cells and spiral arterioles as well as localize to the trophoblast cells during early
266 pregnancy—suggesting a role for *CTTN* in cytoskeletal remodeling of the maternal-fetal interface during
267 early pregnancy^{85,86}. While neither *CTTN* nor *PPFIA1* have been implicated in sPTB, they are both linked
268 to cell adhesion and there is evidence that decreased adherence of maternal and fetal membrane layers is
269 involved in parturition⁸⁷. The accelerated evolution associated with variants in this region is also
270 consistent with the rapid diversification of the placenta within eutherians^{88–90}. While the proteins *CTTN*
271 and *PPFIA1* are highly conserved across mammals, the accelerated evolution detected in association with
272 rs1061328 may be linked to the functionally important and diverse splice variants of both proteins^{74,91}.
273 Accelerated evolution has previously been detected in the birth timing-associated genes *FSHR*⁴⁷ and
274 *PLA2G4C*⁹². It has been hypothesized that human and/or primate-specific adaptations, such as bipedalism,
275 have resulted in the accelerated evolution of birth-timing phenotypes along these lineages^{2,93,94}.
276 Accelerated evolution has also been implicated in other complex disorders—especially those like
277 schizophrenia^{95,96} and autism⁹⁷ which affect the brain, another organ that is thought to have undergone
278 adaptive evolution in the human lineage.

279 **Group D: Balanced Polymorphism/Balancing Selection**

280 Variants in Group D generally had higher than expected values of beta score or an older allele age than
281 expected, which is consistent with evolutionary signatures of balancing selection (Figure 2). Beta score is
282 a measure of long-term balancing selection within the human lineage³³. Allele age is measured as the time
283 to most recent common ancestor (TMRCA) in thousands of generations since present based on 54
284 unrelated individuals, which was obtained from ARGweaver³⁴. There are nine genomic regions in group
285 D, of which three have a significantly ($p < 0.05$) higher beta score than expected, three have a significantly
286 older ($p < 0.05$) than expected TMRCA, and three have older TMRCA but are not significant. The derived
287 alleles in this group have an average derived allele frequency across all populations of 0.44 (Figure
288 3C). There are 292 variants in this group; nearly all of these variants are intronic (274/292; Figure 3A) and
289 there is evidence of regulatory binding for 11 variants (regulome DB score of 1 or 2; Figure 3B). GTEx

290 analysis supports the regulatory role of a number of variants—266 of 271 variants are an eQTL in at least
291 one tissue (Figure 3D). For the genomic region associated with the lead variant rs10932774 there are 26
292 additional variants which are eQTLs for an average of 80 unique tissue/gene combinations. eQTL
293 analysis detects at least one expression change in the uterus in all but five of these variants.

294 The variant rs10932774 is located within the 2nd of nine introns in the gene *PNKD* (also known as
295 myofibrillogenesis regulator 1), which is the causal gene in the neurological movement disorder
296 paroxysmal nonkinesigenic dyskinesia (PNKD)⁹⁸. This variant has a significant value for both TMRCAs
297 and beta score. The G allele at this locus is associated with an increased risk of sPTB (OR: 1.11, adjusted
298 p-value 8.85×10^{-5})³² and is the major allele in all the populations examined (Figure 4D). Supporting the
299 interpretation of long-term balancing selection, this polymorphism is also present in the great apes. This
300 variant is associated with the expression of five genes in 43 tissues for a total of 73 gene/tissue
301 combinations in the GTEx database. Additionally, the *PNKD* gene is up-regulated in severely
302 preeclamptic placentas⁹⁹ and in PNKD patients pregnancy is associated with changes in the frequency or
303 severity of PNKD attacks^{100–102}. Expression changes in the Transmembrane BAX Inhibitor Motif-
304 Containing Protein 1 gene (*TMBIM1*) and the Actin Related Protein 2/3 Complex Subunit 2 gene
305 (*ARPC2*) are also associated with this variant. *TMBIM1* is a cell death regulator¹⁰³ with no known role in
306 pregnancy. Methylation of *TMBIM1*, however, is altered in the offspring of mothers with Type 1
307 Diabetes¹⁰⁴. The gene *ARPC2* is a subunit of the Arp2/3 complex which controls actin polymerization and
308 is also highly conserved^{105,106}. The complex is important for early embryo development and
309 preimplantation in pigs and mice^{107,108}. *ARPC2* expression has been identified in the BeWo trophoblastic
310 cell line used to investigate placental function¹⁰⁹ and is subject to RNA editing in placentas associated
311 with intrauterine growth restriction/small for gestational age (SGA)¹¹⁰. Overall, genes associated with the
312 variant rs10932774 (*PNKD*, *TMBIM1* and *ARPC2*) show long-term evolutionary conservation consistent
313 with a signature of balancing selection and prior research suggests links to pregnancy through a variety of
314 mechanisms. The identification of balancing selection acting on sPTB-associated genomic regions is

315 consistent with the critical role of the immune system, which often experiences balancing
316 selection^{33,111,112}, in establishing and maintaining pregnancy¹¹³.

317 **The largest group of variants consists of a variety of evolutionary signatures**

318 The final group, group E, contained the remaining genomic regions in clusters E1, E2, E3 and E4 and was
319 associated with a broad range of evolutionary signatures (Figure 2). At least one variant in group E had a
320 significant p-value for every evolutionary measure except for alignment block age. While this group does
321 not reflect the action of a single evolutionary measure or force, over half of the lead variants (39/73) had a
322 significant p-value ($p < 0.05$) for either GERP or XP-EHH. This group also contained 23 of the 33
323 genomic regions with a z-score ($|z| > 1.5$) for population specific iHS (Supp. Table 2). These genomic
324 regions contained a total of 444 linked variants of which 242 are intronic variants, 178 are intergenic
325 variants and the remaining 24 variants are upstream and downstream variants (Figure 4A). This group
326 also contains 19 variants that are likely to affect binding (regulomeDB score of 1 or 2; Fig. 4b). The
327 majority of the derived alleles in this group are minor in Europeans (313/444; Figure 4C). There are also
328 143 variants identified as eQTLs, including 16 expression changes for genes in the uterus (all associated
329 with the variant rs12646130; Figure 4D). Interestingly, this group contained variants linked to the
330 *EEFSEC*, *ADCY5*, and *WNT4* genes, which have been previously associated with gestational duration or
331 preterm birth³².

332 The variant rs8126001 is located in the 5' UTR of the opioid related nociception receptor 1 or nociception
333 opioid receptor (*OPRL1* or *NOP-R*) gene which may be involved in myometrial contractions during
334 delivery^{114,115}. This variant has signatures of positive selection as detected by the integrated haplotype
335 score (iHS) within the African population (Supp. Table 2). The T allele at this locus is protective for
336 sPTB (effect: 0.896; adjusted p-value 4.04×10^{-5})³² and arose in the human lineage. The protective allele
337 has a relatively low frequency in the African population and is located in a region with low haplotype
338 diversity (Figure 4E). This locus is also associated with expression of *OPRL1* in tissues like the brain,
339 aorta and esophagus (Figure 4E). The gene *OPRL1* is a receptor for the endogenous peptide nociceptin

340 (N/OFQ) which is derived from prenocicpetin (PNOC). There is evidence that nociception and its
341 receptor may play a role in pregnancy. N/OFQ and PNOC were detected in rat and human pregnant
342 myometrial tissues³² and *OPRL1* was detected in rat myometrium.^{114,116} Additionally, *PNOC* mRNA
343 levels are significantly higher in preterm uterine samples in humans and can elicit myometrial relaxation
344 *in vitro*^{115,116}. It is therefore likely that nociceptin and *OPRL1* are involved in the perception of pain
345 during delivery and the initiation of delivery. While a single mode of evolution does not characterize
346 group E, the high frequency of genomic regions with significant XP-EHH or population specific iHS
347 values (40/73 genomic regions) suggests that population-specific evolutionary forces may be at play in
348 this group. The sPTB GWAS and population-specific evolutionary measures were conducted in women of
349 European ancestry but we know that sPTB risk varies with genomic background^{117,118}. Therefore, this
350 group also suggests that individual populations experience a different mosaic of evolutionary forces on
351 pregnancy phenotypes.

352 CONCLUSIONS

353 In this study, we developed an approach to test for signatures of diverse evolutionary forces and applied it
354 to sPTB-associated genomic regions. This approach explicitly accounts for MAF and LD in trait-
355 associated genomic regions. We find evolutionary conservation, excess population differentiation,
356 accelerated evolution, and balanced polymorphisms in 120 of the 215 sPTB-associated genomic regions.
357 Annotation of these regions using existing databases and literature suggest plausible functional links to
358 pregnancy phenotypes, bolstering our confidence that these regions contribute to sPTB risk. These results
359 suggest that no single evolutionary force is responsible for shaping the genetic architecture of sPTB;
360 rather, sPTB has been influenced by a diverse mosaic of evolutionary forces. We hypothesize that the
361 same is likely to be true of other complex human traits and disorders; future investigations that test for
362 signatures of multiple evolutionary forces, such as ours, promise to elucidate the degree to which the
363 landscape of evolutionary forces varies across disorders.

364 **METHODS**

365 **Deriving independent genomic regions associated with sPTB from GWAS summary statistics**

366 To evaluate evolutionary history of sPTB on distinct regions of the human genome, we identified
367 genomic regions from the GWAS summary statistics. Using PLINK1.9b
368 (pngu.mgh.harvard.edu/purcell/plink/)¹⁰², the top 10,000 variants associated with sPTB from Zhang et.
369 al.³¹ were clumped based on LD using default settings except requiring a p-value $\leq 10E-4$ for lead
370 variants and variants in LD with lead variants. We used this liberal p-value threshold to increase the
371 number of sPTB-associated variants evaluated. Although this will increase the number of false
372 positive variants associated with sPTB, we anticipate that these false positive variants will not
373 have statistically significant evolutionary signals using our approach to detect evolutionary
374 forces. This is because the majority of the genome is neutrally evolving and our approach aims to
375 detect deviation from this genomic background. Additionally, it is possible that the lead variant
376 (variant with the lowest p-value) could tag the true variant associated with sPTB within an LD block.
377 Therefore, we defined an independent sPTB-associated genomic region to include the lead and LD
378 ($r^2 > 0.9$, p-value $\leq 10E-4$) sPTB variants. This resulted in 215 independent lead variants within an sPTB-
379 associated genomic region.

380 **Creating matched control regions for each sPTB-associated genomic regions**

381 We detected evolutionary signatures at genomic regions associated with sPTB by comparing them to
382 matched control sets. Since evolutionary measures are influenced by LD and allele frequencies and these
383 also influence power in GWAS, we generated control regions matched for these attributes for observed
384 sPTB-associated genomic regions. First, for each lead variant we identified 5,000 control variants
385 matched on minor allele frequency ($\pm 5\%$), LD ($r^2 > 0.9$, $\pm 10\%$ number of LD buddies), gene density
386 ($\pm 500\%$) and distance to nearest gene ($\pm 500\%$) using SNPSNAP¹¹⁹, which derives controls variants
387 from a quality controlled phase 3 100 Genomes (1KG) data, with default settings for all other parameters

388 and the hg19/GRCh37 genome assembly. For each control variant, we randomly selected an equal
389 number of variants in LD ($r^2 > 0.9$) as sPTB-associated variants in LD with the corresponding lead variant.
390 If no matching control variant existed, we relaxed the LD required to $r^2 = 0.6$. If still no match was found,
391 we treated this as a missing value. For all LD calculations, control variants and downstream evolutionary
392 measure analyses, the European super-population from phase 3 1KG¹²⁰ was used after removing duplicate
393 variants.

394 **Evolutionary measures**

395 To characterize the evolutionary dynamics at each sPTB-associated region, we evaluated diverse
396 evolutionary measures for diverse modes of selection and allele history across each sPTB-associated
397 genomic region. Evolutionary measures were either calculated or pre-calculated values were downloaded
398 for all control and sPTB-associated variants. Pairwise Weir and Cockerham's F_{ST} values between
399 European, East Asian, and African super populations from 1KG were calculated using VCFTools
400 (v0.1.14)¹²¹. Evolutionary measures of positive selection, iHS, XP-EHH, and iES, were calculated from
401 the 1KG data using rehh 2.0¹²². Beta score, a measure of balancing selection, was calculated using
402 BetaScan software³³. Alignment block age was calculated using 100-way multiple sequence alignment¹²³
403 to measure the age of alignment blocks defined by the oldest most recent common ancestor. The
404 remaining measures were downloaded from publicly available sources: phyloP and phastCons 100 way
405 alignment from UCSC genome browser¹²⁴; LINSIGHT³⁵; and allele age (time to most common recent
406 ancestor from ARGWEAVER)³⁴. Due to missing values, the exact number of control regions varied by
407 sPTB-associated region and evolutionary measure. We first marked any control set that did not match at
408 least 90% of the required variants for a given sPTB-associated region, then any sPTB-associated region
409 with $\geq 60\%$ marked control regions were removed for that specific evolutionary measure. iHS was not
410 included in Figure 2 because of large amounts of missing data for up to 50% of genomic regions
411 evaluated.

412 **Detecting significant differences in evolutionary measures by comparing to control distributions**

413 For each sPTB-associated genomic region for a specific evolutionary measure, we took the median value
414 of the evolutionary measure across all its variants and compared it to the distribution of median values
415 from the corresponding control regions. Statistical significance for each sPTB-associated region was
416 evaluated by comparing the median value of the evolutionary measure to the distribution of the median
417 value of the control regions. To obtain the p-value, we calculated the number of control regions with a
418 median value that are equal to or greater the median value for the PTB region. Since allele age (TMRCA
419 from ARGweaver), PhyloP, and alignment block age are bi-directional measures, we calculated two-
420 tailed p-values; all other evolutionary measures used one-tailed p-values. To compare evolutionary
421 measures whose scales differ substantially, we calculated a z-score for each region per measure. These z-
422 scores were hierarchically clustered across all regions and measures. Clusters were defined by a branch
423 length cutoff of seven. These clusters were then grouped and annotated by the dominant evolutionary
424 measure through manual inspection to highlight the main evolutionary trend(s).

425 **Annotation of variants in sPTB-associated regions**

426 To understand functional differences between groups and genomic regions we collected annotations for
427 variants in sPTB-associated regions from publicly available databases. Evidence for regulatory function
428 for individual variants was obtained from RegulomeDB v1.1 (accessed 1/11/19)¹²⁵. From this we
429 extracted the following information: total promotor histone marks, total enhancer histone marks, total
430 DNase 1 sensitivity, total predicted proteins bound, total predicted motifs changed, and regulomeDB
431 score. Variants were identified as expression quantitative trait loci (eQTLs) using the Genotype-Tissue
432 Expression (GTEx) project data (dbGaP Accession phs000424.v7.p2 accessed 1/15/19). Variants were
433 mapped to GTEx annotations based on rs number and then the GTEx annotations were used to obtain
434 eQTL information. For each locus, we obtained the tissues in which the locus was an eQTL, the genes for
435 which the locus affected expression (in any tissue), and the total number times the locus was identified as
436 an eQTL. Functional variant effects were annotated with the Ensembl Variant Effect Predictor (VEP;

437 accessed 1/17/19) based on rs number¹²⁶. Population-based allele frequencies were obtained from the
438 1KG phase3 data for the African (excluding related African individuals; Supplementary Table 3), East
439 Asian, and European populations¹²⁰.

440 To infer the history of the alleles at each locus across mammals, we created a mammalian alignment at
441 each locus and inferred the ancestral states. That mammalian alignment was built using data from the
442 sPTB GWAS³² (risk variant identification), the UCSC Table Browser¹²³ (30 way mammalian alignment),
443 the 1KG phase 3¹²⁰ data (human polymorphism data) and the Great Ape Genome project (great ape
444 polymorphisms)¹²⁷—which reference different builds of the human genome. To access data constructed
445 across multiple builds of the human genome, we used Ensembl biomart release 97¹²⁸ and the biomaRt R
446 package^{129,130} to obtain the position of variants in hg38, hg19, and hg18 based on RefSNP (rs) number¹³¹.
447 Alignments with more than one gap position were discarded due to uncertainty in the alignment. All
448 variant data were checked to ensure that each dataset reported polymorphisms in reference to the same
449 strand. Parsimony reconstruction was conducted along a phylogenetic tree generated from the TimeTree
450 database¹³². Ancestral state reconstruction for each allele was conducted in R using parsimony estimation
451 in the phangorn package¹³³. Five character-states were used in the ancestral state reconstruction: one for
452 each base and a fifth for gap. Haplotype blocks containing the variant of interest were identified using
453 Plink (v1.9b_5.2) to create blocks from the 1KG phase3 data. Binary haplotypes were then generated for
454 each of the three populations using the IMPUTE function of vcftools (v0.1.15.) Median joining
455 networks¹³⁴ were created using PopART¹³⁵.

456 **URLs:**

Evolutionary Measures	Source
PhyloP	http://hgdownload.cse.ucsc.edu/goldenPath/hg19/phyloP100way/
PhastCons	http://hgdownload.cse.ucsc.edu/goldenPath/hg19/phastCons100way/
LINSIGHT	http://compugen.cshl.edu/~yihuang/LINSIGHT
GERP	http://genome.ucsc.edu/cgi-bin/hgTrackUi?db=hg19&g=allHg19RS_BW
Weir and Cockerham's F_{ST}	calculated with VCFTools (v0.1.14, https://vcftools.github.io/index.html) using Thousand Genomes Phase 3 (http://www.internationalgenome.org/)

Integrated haplotype score (iHS)	
Cross-population EHH (XP-EHH)	calculated with rehh (v2.0, https://cran.r-project.org/web/packages/rehh/index.html) using 1000 Genomes Project (http://www.internationalgenome.org/)
Integrated site-specific EHH (iES)	
Beta Score	calculated with BetaScan (https://github.com/ksiewert/BetaScan) using 1000 Genomes Project (http://www.internationalgenome.org/)
Alignment Block Age	calculated from 100-way species alignment obtained from UCSC (http://hgdownload.cse.ucsc.edu/goldenpath/hg19/multiz100way/)
TMRCAs from ARGWEAVER	http://compgen.cshl.edu/ARGweaver/CG_results/download/

457

458 **Data Availability**

459 All the data used in this study were obtained from the public domain (see the URLs above) or deposited
460 in a figshare repository to be made public upon publication.

461 **Code Availability**

462 All scripts used to measure evolutionary signatures and generate figures are publicly accessible in a
463 figshare repository to be made public upon publication.

464

465 **References**

- 466 1. Eidem, H. R., McGary, K. L., Capra, J. A., Abbot, P. & Rokas, A. The transformative potential of
467 an integrative approach to pregnancy. *Placenta* **57**, 204–215 (2017).
- 468 2. Abbot, P. & Rokas, A. Mammalian pregnancy. *Current Biology* (2017).
469 doi:10.1016/j.cub.2016.10.046
- 470 3. Moon, J. M., Capra, J. A., Abbot, P. & Rokas, A. Immune Regulation in Eutherian Pregnancy:
471 Live Birth Coevolved with Novel Immune Genes and Gene Regulation. *BioEssays* (2019).
472 doi:10.1002/bies.201900072
- 473 4. Rosenberg, K. & Trevathan, W. Bipedalism and human birth: The obstetrical dilemma revisited.
474 *Evol. Anthropol. Issues, News, Rev.* **4**, 161–168 (1995).
- 475 5. Rosenberg, K. R. The evolution of modern human childbirth. *Am. J. Phys. Anthropol.* (1992).
476 doi:10.1002/ajpa.1330350605
- 477 6. Washburn, S. L. Tools and human evolution. *Sci Am* **203**, 63–75 (1960).
- 478 7. Krogman, W. M. The scars of human evolution. *Sci. Am.* **185**, 54–57 (1951).
- 479 8. Dunsworth, H. M., Warrener, A. G., Deacon, T., Ellison, P. T. & Pontzer, H. Metabolic hypothesis
480 for human altriciality. *Proc Natl Acad Sci U S A* **109**, 15212–15216 (2012).
- 481 9. Romero, R., Dey, S. K. & Fisher, S. J. Preterm labor: One syndrome, many causes. *Science*
482 (2014). doi:10.1126/science.1251816
- 483 10. Martin, J. A., Hamilton, B. E. & Osterman, M. J. K. Births in the United States, 2016. *NCHS Data*
484 *Brief* (2017).
- 485 11. Blencowe, H. *et al.* National, regional, and worldwide estimates of preterm birth rates in the year
486 2010 with time trends since 1990 for selected countries: A systematic analysis and implications.
487 *Lancet* (2012). doi:10.1016/S0140-6736(12)60820-4
- 488 12. Goldenberg, R. L., Culhane, J. F., Iams, J. D. & Romero, R. Epidemiology and causes of preterm
489 birth. *The Lancet* (2008). doi:10.1016/S0140-6736(08)60074-4
- 490 13. Esplin, M. S. Overview of spontaneous preterm birth: A complex and multifactorial phenotype. in
491 *Clinical Obstetrics and Gynecology* (2014). doi:10.1097/GRF.0000000000000037
- 492 14. Chang, H. H. *et al.* Preventing preterm births: Analysis of trends and potential reductions with
493 interventions in 39 countries with very high human development index. *Lancet* (2013).
494 doi:10.1016/S0140-6736(12)61856-X
- 495 15. Bezold, K. Y., Karjalainen, M. K., Hallman, M., Teramo, K. & Muglia, L. J. The genomics of
496 preterm birth: From animal models to human studies. *Genome Medicine* (2013).
497 doi:10.1186/gm438
- 498 16. Moutquin, J. M. Classification and heterogeneity of preterm birth. in *BJOG: An International*
499 *Journal of Obstetrics and Gynaecology* (2003). doi:10.1016/S1470-0328(03)00021-1
- 500 17. Barros, F. C. *et al.* The Distribution of Clinical Phenotypes of Preterm Birth Syndrome. *JAMA*
501 *Pediatr.* (2015). doi:10.1001/jamapediatrics.2014.3040
- 502 18. Ananth, C. V. & Vintzileos, A. M. Epidemiology of preterm birth and its clinical subtypes.
503 *Journal of Maternal-Fetal and Neonatal Medicine* (2006). doi:10.1080/14767050600965882

- 504 19. Henderson, J. J., McWilliam, O. A., Newnham, J. P. & Pennell, C. E. Preterm birth aetiology
505 2004-2008. Maternal factors associated with three phenotypes: Spontaneous preterm labour,
506 preterm pre-labour rupture of membranes and medically indicated preterm birth. *J. Matern.*
507 *Neonatal Med.* (2012). doi:10.3109/14767058.2011.597899
- 508 20. Boyd, H. A. *et al.* Maternal Contributions to Preterm Delivery. *Am. J. Epidemiol.* (2009).
509 doi:10.1093/aje/kwp324
- 510 21. Kistka, Z. A. F. *et al.* Heritability of parturition timing: an extended twin design analysis. *Am. J.*
511 *Obstet. Gynecol.* (2008). doi:10.1016/j.ajog.2007.12.014
- 512 22. Plunkett, J. *et al.* Mother's genome or maternally-inherited genes acting in the fetus influence
513 gestational age in familial preterm birth. *Hum. Hered.* (2009). doi:10.1159/000224641
- 514 23. York, T. P. *et al.* Fetal and maternal genes' influence on gestational age in a quantitative genetic
515 analysis of 244,000 swedish births. *Am. J. Epidemiol.* (2013). doi:10.1093/aje/kwt005
- 516 24. Clausson, B., Lichtenstein, P. & Cnattingius, S. Genetic influence on birthweight and gestational
517 length determined by studies in offspring of twins. *BJOG An Int. J. Obstet. Gynaecol.* (2000).
518 doi:10.1111/j.1471-0528.2000.tb13234.x
- 519 25. Kjeldbjerg, A. L., Villesen, P., Aagaard, L. & Pedersen, F. S. Gene conversion and purifying
520 selection of a placenta-specific ERV-V envelope gene during simian evolution. *BMC Evol Biol* **8**,
521 266 (2008).
- 522 26. Hiby, S. E. *et al.* Maternal KIR in Combination with Paternal HLA-C2 Regulate Human Birth
523 Weight. *J. Immunol.* (2014). doi:10.4049/jimmunol.1400577
- 524 27. Guinan, K. J. *et al.* Signatures of natural selection and coevolution between killer cell
525 immunoglobulin-like receptors (KIR) and HLA class I genes. *Genes Immun.* (2010).
526 doi:10.1038/gene.2010.9
- 527 28. Phillips, J. B., Abbot, P. & Rokas, A. Is preterm birth a human-specific syndrome? *Evol. Med.*
528 *Public Heal.* (2015). doi:10.1093/emph/eov010
- 529 29. Chen, C. *et al.* The human progesterone receptor shows evidence of adaptive evolution associated
530 with its ability to act as a transcription factor. *Mol. Phylogenet. Evol.* (2008).
531 doi:10.1016/j.ympev.2007.12.026
- 532 30. Li, J. *et al.* Natural Selection Has Differentiated the Progesterone Receptor among Human
533 Populations. *Am J Hum Genet* **103**, 45–57 (2018).
- 534 31. Newnham, J. P. *et al.* Strategies to prevent preterm birth. *Frontiers in Immunology* (2014).
535 doi:10.3389/fimmu.2014.00584
- 536 32. Zhang, G., Jacobsson, B. & Muglia, L. J. Genetic Associations with Spontaneous Preterm Birth.
537 *N. Engl. J. Med.* **377**, 2401–2402 (2017).
- 538 33. Siewert, K. M. & Voight, B. F. Detecting Long-Term Balancing Selection Using Allele Frequency
539 Correlation. *Mol Biol Evol* **34**, 2996–3005 (2017).
- 540 34. Rasmussen, M. D., Hubisz, M. J., Gronau, I. & Siepel, A. Genome-Wide Inference of Ancestral
541 Recombination Graphs. *PLoS Genet.* (2014). doi:10.1371/journal.pgen.1004342
- 542 35. Huang, Y. F., Gulko, B. & Siepel, A. Fast, scalable prediction of deleterious noncoding variants
543 from functional and population genomic data. *Nat. Genet.* (2017). doi:10.1038/ng.3810

- 544 36. Akey, J. M. Constructing genomic maps of positive selection in humans: Where do we go from
545 here? *Genome Research* (2009). doi:10.1101/gr.086652.108
- 546 37. Pybus, M. *et al.* 1000 Genomes Selection Browser 1.0: A genome browser dedicated to signatures
547 of natural selection in modern humans. *Nucleic Acids Res.* (2014). doi:10.1093/nar/gkt1188
- 548 38. Vitti, J. J., Grossman, S. R. & Sabeti, P. C. Detecting Natural Selection in Genomic Data. *Annu.*
549 *Rev. Genet.* (2013). doi:10.1146/annurev-genet-111212-133526
- 550 39. Stern, A. J. & Nielsen, R. Detecting Natural Selection. *Handb. Stat. Genomics 4e 2V SET* 340–397
551 (2019).
- 552 40. Booker, T. R., Jackson, B. C. & Keightley, P. D. Detecting positive selection in the genome. *BMC*
553 *Biology* (2017). doi:10.1186/s12915-017-0434-y
- 554 41. Visscher, P. M. *et al.* 10 Years of GWAS Discovery: Biology, Function, and Translation.
555 *American Journal of Human Genetics* (2017). doi:10.1016/j.ajhg.2017.06.005
- 556 42. Guo, J. *et al.* Global genetic differentiation of complex traits shaped by natural selection in
557 humans. *Nat. Commun.* (2018). doi:10.1038/s41467-018-04191-y
- 558 43. Byars, S. G. *et al.* Genetic loci associated with coronary artery disease harbor evidence of
559 selection and antagonistic pleiotropy. *PLoS Genet.* (2017). doi:10.1371/journal.pgen.1006328
- 560 44. O'Connor, L. J. *et al.* Extreme Polygenicity of Complex Traits Is Explained by Negative
561 Selection. *Am. J. Hum. Genet.* (2019). doi:10.1016/j.ajhg.2019.07.003
- 562 45. Zeng, J. *et al.* Signatures of negative selection in the genetic architecture of human complex traits.
563 *Nat. Genet.* (2018). doi:10.1038/s41588-018-0101-4
- 564 46. Guo, J., Yang, J. & Visscher, P. M. Leveraging GWAS for complex traits to detect signatures of
565 natural selection in humans. *Current Opinion in Genetics and Development* (2018).
566 doi:10.1016/j.gde.2018.05.012
- 567 47. Plunkett, J. *et al.* An evolutionary genomic approach to identify genes involved in human birth
568 timing. *PLoS Genet* **7**, e1001365 (2011).
- 569 48. Guinan, K. J. *et al.* Signatures of natural selection and coevolution between killer cell
570 immunoglobulin-like receptors (KIR) and HLA class I genes. *Genes Immun* **11**, 467–478 (2010).
- 571 49. Gu, T. P. *et al.* The role of Tet3 DNA dioxygenase in epigenetic reprogramming by oocytes.
572 *Nature* **477**, 606–610 (2011).
- 573 50. Tsukada, Y., Akiyama, T. & Nakayama, K. I. Maternal TET3 is dispensable for embryonic
574 development but is required for neonatal growth. *Sci Rep* **5**, 15876 (2015).
- 575 51. Rakoczy, J. *et al.* Dynamic expression of TET1, TET2, and TET3 dioxygenases in mouse and
576 human placentas throughout gestation. *Placenta* **59**, 46–56 (2017).
- 577 52. Sober, S. *et al.* Extensive shift in placental transcriptome profile in preeclampsia and placental
578 origin of adverse pregnancy outcomes. *Sci Rep* **5**, 13336 (2015).
- 579 53. Fitzgerald, E., Boardman, J. P. & Drake, A. J. Preterm Birth and the Risk of Neurodevelopmental
580 Disorders - Is There a Role for Epigenetic Dysregulation? *Curr Genomics* **19**, 507–521 (2018).
- 581 54. Zelko, I. N., Zhu, J. & Roman, J. Maternal undernutrition during pregnancy alters the epigenetic
582 landscape and the expression of endothelial function genes in male progeny. *Nutr Res* **61**, 53–63

- 583 (2019).
- 584 55. Akahori, H., Guindon, S., Yoshizaki, S. & Muto, Y. Molecular evolution of the TET gene family
585 in mammals. *Int. J. Mol. Sci.* (2015). doi:10.3390/ijms161226110
- 586 56. Gazal, S. *et al.* Linkage disequilibrium-dependent architecture of human complex traits shows
587 action of negative selection. *Nat. Genet.* (2017). doi:10.1038/ng.3954
- 588 57. Kistka, Z. A. *et al.* Racial disparity in the frequency of recurrence of preterm birth. *Am J Obs.*
589 *Gynecol* **196**, 131 e1–6 (2007).
- 590 58. Muglia, L. J. & Katz, M. The enigma of spontaneous preterm birth. *N Engl J Med* **362**, 529–535
591 (2010).
- 592 59. Jung, K. H. *et al.* Associations of vitamin d binding protein gene polymorphisms with the
593 development of peripheral arthritis and uveitis in ankylosing spondylitis. *J Rheumatol* **38**, 2224–
594 2229 (2011).
- 595 60. Muindi, J. R. *et al.* Serum vitamin D metabolites in colorectal cancer patients receiving
596 cholecalciferol supplementation: correlation with polymorphisms in the vitamin D genes. *Horm*
597 *Cancer* **4**, 242–250 (2013).
- 598 61. Wei, S. Q., Qi, H. P., Luo, Z. C. & Fraser, W. D. Maternal vitamin D status and adverse pregnancy
599 outcomes: a systematic review and meta-analysis. *J Matern Fetal Neonatal Med* **26**, 889–899
600 (2013).
- 601 62. Bodnar, L. M., Platt, R. W. & Simhan, H. N. Early-pregnancy vitamin D deficiency and risk of
602 preterm birth subtypes. *Obs. Gynecol* **125**, 439–447 (2015).
- 603 63. Qin, L. L., Lu, F. G., Yang, S. H., Xu, H. L. & Luo, B. A. Does Maternal Vitamin D Deficiency
604 Increase the Risk of Preterm Birth: A Meta-Analysis of Observational Studies. *Nutrients* **8**, (2016).
- 605 64. Zhou, S. S., Tao, Y. H., Huang, K., Zhu, B. B. & Tao, F. B. Vitamin D and risk of preterm birth:
606 Up-to-date meta-analysis of randomized controlled trials and observational studies. *J Obs.*
607 *Gynaecol Res* **43**, 247–256 (2017).
- 608 65. Liong, S., Di Quinzio, M. K., Fleming, G., Permezel, M. & Georgiou, H. M. Is vitamin D binding
609 protein a novel predictor of labour? *PLoS One* **8**, e76490 (2013).
- 610 66. D’Silva, A. M., Hyett, J. A. & Coorsen, J. R. Proteomic analysis of first trimester maternal serum
611 to identify candidate biomarkers potentially predictive of spontaneous preterm birth. *J. Proteomics*
612 (2018). doi:10.1016/j.jprot.2018.02.002
- 613 67. Bodnar, L. M. & Simhan, H. N. Vitamin D may be a link to black-white disparities in adverse
614 birth outcomes. *Obs. Gynecol Surv* **65**, 273–284 (2010).
- 615 68. Burris, H. H. *et al.* Plasma 25-hydroxyvitamin D during pregnancy and small-for-gestational age
616 in black and white infants. *Ann Epidemiol* **22**, 581–586 (2012).
- 617 69. Reeves, I. V. *et al.* Vitamin D deficiency in pregnant women of ethnic minority: A potential
618 contributor to preeclampsia. *J. Perinatol.* (2014). doi:10.1038/jp.2014.91
- 619 70. Ramagopalan, S. V. *et al.* A ChIP-seq defined genome-wide map of vitamin D receptor binding:
620 Associations with disease and evolution. *Genome Res.* (2010). doi:10.1101/gr.107920.110
- 621 71. Jablonski, N. G. & Chaplin, G. The roles of vitamin D and cutaneous vitamin D production in
622 human evolution and health. *International Journal of Paleopathology* (2018).

- 623 doi:10.1016/j.ijpp.2018.01.005
- 624 72. Hollis, B. W. & Wagner, C. L. New insights into the vitamin D requirements during pregnancy.
625 *Bone Res* **5**, 17030 (2017).
- 626 73. Carithers, L. J. *et al.* A Novel Approach to High-Quality Postmortem Tissue Procurement: The
627 GTEx Project. *Biopreserv. Biobank.* (2015). doi:10.1089/bio.2015.0032
- 628 74. Zurner, M. & Schoch, S. The mouse and human Liprin-alpha family of scaffolding proteins:
629 Genomic organization, expression profiling and regulation by alternative splicing. *Genomics* **93**,
630 243–253 (2009).
- 631 75. Asperti, C., Pettinato, E. & de Curtis, I. Liprin-alpha1 affects the distribution of low-affinity beta1
632 integrins and stabilizes their permanence at the cell surface. *Exp Cell Res* **316**, 915–926 (2010).
- 633 76. Astro, V., Asperti, C., Cangì, M. G., Doglioni, C. & de Curtis, I. Liprin-alpha1 regulates breast
634 cancer cell invasion by affecting cell motility, invadopodia and extracellular matrix degradation.
635 *Oncogene* **30**, 1841–1849 (2011).
- 636 77. de Curtis, I. Function of liprins in cell motility. *Exp Cell Res* **317**, 1–8 (2011).
- 637 78. Yang, J. T., Rayburn, H. & Hynes, R. O. Cell adhesion events mediated by alpha 4 integrins are
638 essential in placental and cardiac development. *Development* **121**, 549–560 (1995).
- 639 79. Burrows, T. D., King, A. & Loke, Y. W. Trophoblast migration during human placental
640 implantation. *Hum Reprod Updat.* **2**, 307–321 (1996).
- 641 80. Mincheva-Nilsson, L. & Baranov, V. The role of placental exosomes in reproduction. *Am J*
642 *Reprod Immunol* **63**, 520–533 (2010).
- 643 81. Paidas, M. J. *et al.* A genomic and proteomic investigation of the impact of preimplantation factor
644 on human decidual cells. *Am J Obs. Gynecol* **202**, 459 e1–8 (2010).
- 645 82. Weed, S. A. & Parsons, J. T. Cortactin: coupling membrane dynamics to cortical actin assembly.
646 *Oncogene* **20**, 6418–6434 (2001).
- 647 83. van Rossum, A. G., Moolenaar, W. H. & Schuurin, E. Cortactin affects cell migration by
648 regulating intercellular adhesion and cell spreading. *Exp Cell Res* **312**, 1658–1670 (2006).
- 649 84. Clark, E. S., Whigham, A. S., Yarbrough, W. G. & Weaver, A. M. Cortactin is an essential
650 regulator of matrix metalloproteinase secretion and extracellular matrix degradation in
651 invadopodia. *Cancer Res* **67**, 4227–4235 (2007).
- 652 85. Paule, S. G., Airey, L. M., Li, Y., Stephens, A. N. & Nie, G. Proteomic approach identifies
653 alterations in cytoskeletal remodelling proteins during decidualization of human endometrial
654 stromal cells. *J Proteome Res* **9**, 5739–5747 (2010).
- 655 86. Paule, S., Li, Y. & Nie, G. Cytoskeletal remodelling proteins identified in fetal-maternal interface
656 in pregnant women and rhesus monkeys. *J Mol Histol* **42**, 161–166 (2011).
- 657 87. Strohl, A. *et al.* Decreased adherence and spontaneous separation of fetal membrane layers--
658 amnion and choriodecidua--a possible part of the normal weakening process. *Placenta* **31**, 18–24
659 (2010).
- 660 88. Ford, S. P. Embryonic and fetal development in different genotypes in pigs. *J. Reprod. Fertil.*
661 *Suppl.* (1997).

- 662 89. Mossman, H. W. Comparative morphogenesis of the fetal membranes and accessory uterine
663 structures. *Placenta* (1991). doi:10.1016/0143-4004(91)90504-9
- 664 90. Chuong, E. B., Hannibal, R. L., Green, S. L. & Baker, J. C. Evolutionary perspectives into
665 placental biology and disease. *Applied and Translational Genomics* (2013).
666 doi:10.1016/j.atg.2013.07.001
- 667 91. van Rossum, A. G. S. H., Schuurings-Scholtes, E., van Buuren-van Seggelen, V., Kluin, P. M. &
668 Schuurings, E. Comparative genome analysis of cortactin and HS1: The significance of the F-actin
669 binding repeat domain. *BMC Genomics* (2005). doi:10.1186/1471-2164-6-15
- 670 92. Plunkett, J. *et al.* Primate-specific evolution of noncoding element insertion into PLA2G4C and
671 human preterm birth. *BMC Med. Genomics* (2010). doi:10.1186/1755-8794-3-62
- 672 93. Rosenberg, K. & Trevathan, W. Birth, obstetrics and human evolution. *BJOG: An International
673 Journal of Obstetrics and Gynaecology* (2002). doi:10.1046/j.1471-0528.2002.00010.x
- 674 94. Weaver, T. D. & Hublin, J. J. Neandertal birth canal shape and the evolution of human childbirth.
675 *Proc. Natl. Acad. Sci. U. S. A.* (2009). doi:10.1073/pnas.0812554106
- 676 95. Xu, K., Schadt, E. E., Pollard, K. S., Roussos, P. & Dudley, J. T. Genomic and network patterns of
677 schizophrenia genetic variation in human evolutionary accelerated regions. *Mol. Biol. Evol.*
678 (2015). doi:10.1093/molbev/msv031
- 679 96. Srinivasan, S. *et al.* Genetic Markers of Human Evolution Are Enriched in Schizophrenia. *Biol.
680 Psychiatry* (2016). doi:10.1016/j.biopsych.2015.10.009
- 681 97. Polimanti, R. & Gelernter, J. Widespread signatures of positive selection in common risk alleles
682 associated to autism spectrum disorder. *PLoS Genet.* (2017). doi:10.1371/journal.pgen.1006618
- 683 98. Rainier, S. *et al.* Myofibrillogenesis regulator 1 gene mutations cause paroxysmal dystonic
684 choreoathetosis. *Arch. Neurol.* (2004). doi:10.1001/archneur.61.7.1025
- 685 99. Sitras, V. *et al.* Differential Placental Gene Expression in Severe Preeclampsia. *Placenta* (2009).
686 doi:10.1016/j.placenta.2009.01.012
- 687 100. Stefano, E. *et al.* Clinical characteristics of paroxysmal nonkinesigenic dyskinesia in Serbian
688 family with Myofibrillogenesis regulator 1 gene mutation. *Mov. Disord.* (2006).
689 doi:10.1002/mds.21095
- 690 101. Ghezzi, D. *et al.* A family with paroxysmal nonkinesigenic dyskinesias (PNKD): Evidence of
691 mitochondrial dysfunction. *Eur. J. Paediatr. Neurol.* (2015). doi:10.1016/j.ejpn.2014.10.003
- 692 102. Friedman, A. *et al.* Paroxysmal non-kinesigenic dyskinesia caused by the mutation of MR-1 in a
693 large polish kindred. *Eur. Neurol.* (2008). doi:10.1159/000165348
- 694 103. Xu, Q. & Reed, J. C. Bax inhibitor-1, a mammalian apoptosis suppressor identified by functional
695 screening in yeast. *Mol. Cell* (1998). doi:10.1016/S1097-2765(00)80034-9
- 696 104. Gautier, J. F. *et al.* Kidney dysfunction in adult offspring exposed in utero to type 1 diabetes is
697 associated with alterations in genome-wide DNA methylation. *PLoS One* (2015).
698 doi:10.1371/journal.pone.0134654
- 699 105. Welch, M. D., Iwamatsu, A. & Mitchison, T. J. Actin polymerization is induced by Arp2/3 protein
700 complex at the surface of *Listeria monocytogenes*. *Nature* (1997). doi:10.1038/385265a0
- 701 106. Machesky, L. M., Atkinson, S. J., Ampe, C., Vandekerckhove, J. & Pollard, T. D. Purification of a

- 702 cortical complex containing two unconventional actins from *Acanthamoeba* by affinity
703 chromatography on profilin-agarose. *J. Cell Biol.* (1994). doi:10.1083/jcb.127.1.107
- 704 107. Sun, S.-C. *et al.* Actin nucleator Arp2/3 complex is essential for mouse preimplantation embryo
705 development. *Reprod. Fertil. Dev.* (2013). doi:10.1071/rd12011
- 706 108. Li, Y. H. *et al.* Inhibition of the Arp2/3 complex impairs early embryo development of porcine
707 parthenotes. *Animal Cells Syst. (Seoul)*. (2016). doi:10.1080/19768354.2016.1228545
- 708 109. Szklanna, P. B. *et al.* Comparative proteomic analysis of trophoblast cell models reveals their
709 differential phenotypes, potential uses, and limitations. *Proteomics* (2017).
710 doi:10.1002/pmic.201700037
- 711 110. Majewska, M. *et al.* Placenta transcriptome profiling in intrauterine growth restriction (IUGR). *Int.*
712 *J. Mol. Sci.* (2019). doi:10.3390/ijms20061510
- 713 111. Ferrer-Admetlla, A. *et al.* Balancing Selection Is the Main Force Shaping the Evolution of Innate
714 Immunity Genes. *J. Immunol.* (2008). doi:10.4049/jimmunol.181.2.1315
- 715 112. Andrés, A. M. *et al.* Targets of balancing selection in the human genome. *Mol. Biol. Evol.* (2009).
716 doi:10.1093/molbev/msp190
- 717 113. Mor, G. & Cardenas, I. The Immune System in Pregnancy: A Unique Complexity. *American*
718 *Journal of Reproductive Immunology* (2010). doi:10.1111/j.1600-0897.2010.00836.x
- 719 114. Klukovits, A. *et al.* Nociceptin Inhibits Uterine Contractions in Term-Pregnant Rats by Signaling
720 Through Multiple Pathways1. *Biol. Reprod.* (2010). doi:10.1095/biolreprod.109.082222
- 721 115. Gáspár, R., Deák, B. H., Klukovits, A., Ducza, E. & Tekes, K. Effects of Nociceptin and
722 Nocistatin on Uterine Contraction. in *Vitamins and Hormones* (2015).
723 doi:10.1016/bs.vh.2014.10.004
- 724 116. BH, D. Uterus-Relaxing Effects of Nociceptin and Nocistatin: Studies on Preterm and Term-
725 Pregnant Human Myometrium In vitro. *Reprod. Syst. Sex. Disord.* (2013). doi:10.4172/2161-
726 038x.1000117
- 727 117. Manuck, T. A. *et al.* Admixture mapping to identify spontaneous preterm birth susceptibility loci
728 in African Americans. *Obstet. Gynecol.* (2011). doi:10.1097/AOG.0b013e318214e67f
- 729 118. York, T. P., Eaves, L. J., Neale, M. C. & Strauss, J. F. The contribution of genetic and
730 environmental factors to the duration of pregnancy. *American Journal of Obstetrics and*
731 *Gynecology* (2014). doi:10.1016/j.ajog.2013.10.001
- 732 119. Pers, T. H., Timshel, P. & Hirschhorn, J. N. SNPsnip: A Web-based tool for identification and
733 annotation of matched SNPs. *Bioinformatics* (2015). doi:10.1093/bioinformatics/btu655
- 734 120. Genomes Project, C. *et al.* A global reference for human genetic variation. *Nature* **526**, 68–74
735 (2015).
- 736 121. Danecek, P. *et al.* The variant call format and VCFtools. *Bioinformatics* (2011).
737 doi:10.1093/bioinformatics/btr330
- 738 122. Gautier, M., Klassmann, A. & Vitalis, R. rehh 2.0: a reimplementaion of the R package rehh to
739 detect positive selection from haplotype structure. *Mol Ecol Resour* **17**, 78–90 (2017).
- 740 123. Karolchik, D. *et al.* The UCSC Table Browser data retrieval tool. *Nucleic Acids Res.* **32**, D493–
741 D496 (2004).

- 742 124. Kent, W. J. *et al.* The human genome browser at UCSC. *Genome Res* **12**, 996–1006 (2002).
- 743 125. Boyle, A. P. *et al.* Annotation of functional variation in personal genomes using RegulomeDB.
744 *Genome Res* **22**, 1790–1797 (2012).
- 745 126. McLaren, W. *et al.* The Ensembl Variant Effect Predictor. *Genome Biol* **17**, 122 (2016).
- 746 127. Prado-Martinez, J. *et al.* Great ape genetic diversity and population history. *Nature* **499**, 471–475
747 (2013).
- 748 128. Zerbino, D. R. *et al.* Ensembl 2018. *Nucleic Acids Res* **46**, D754–D761 (2018).
- 749 129. Durinck, S. *et al.* BioMart and Bioconductor: a powerful link between biological databases and
750 microarray data analysis. *Bioinformatics* **21**, 3439–3440 (2005).
- 751 130. Durinck, S., Spellman, P. T., Birney, E. & Huber, W. Mapping identifiers for the integration of
752 genomic datasets with the R/Bioconductor package biomaRt. *Nat Protoc* **4**, 1184–1191 (2009).
- 753 131. Lander, E. S. *et al.* Initial sequencing and analysis of the human genome. *Nature* **409**, 860–921
754 (2001).
- 755 132. Kumar, S., Stecher, G., Suleski, M. & Hedges, S. B. TimeTree: A Resource for Timelines,
756 Timetrees, and Divergence Times. *Mol Biol Evol* **34**, 1812–1819 (2017).
- 757 133. Schliep, K. P. phangorn: phylogenetic analysis in R. *Bioinformatics* **27**, 592–593 (2011).
- 758 134. Bandelt, H. J., Forster, P. & Röhl, A. Median-joining networks for inferring intraspecific
759 phylogenies. *Mol. Biol. Evol.* (1999). doi:10.1093/oxfordjournals.molbev.a026036
- 760 135. Leigh, J. W. & Bryant, D. POPART: Full-feature software for haplotype network construction.
761 *Methods Ecol. Evol.* (2015). doi:10.1111/2041-210X.12410
- 762 136. Zhang, G. *et al.* Genetic Associations with Gestational Duration and Spontaneous Preterm Birth.
763 *Obstetrical and Gynecological Survey* (2018). doi:10.1097/01.ogx.0000530434.15441.45
- 764 137. Meunier, J. C. *et al.* Isolation and structure of the endogenous agonist of opioid receptor-like ORL
765 1 receptor. *Nature* (1995). doi:10.1038/377532a0
- 766

767 **Acknowledgements**

768 This work was supported by the National Institutes of Health (grant R35GM127087 to JAC), the
769 Burroughs Wellcome Fund Preterm Birth Initiative (to JAC and AR), and by the March of Dimes through
770 the March of Dimes Prematurity Research Center Ohio Collaborative (to LJM, GZ, PA, JAC, and AR).
771 AA was also supported by NIGMS of the National Institutes of Health under award
772 number T32GM007347. This work was conducted in part using the resources of the Advanced
773 Computing Center for Research and Education at Vanderbilt University. The content is solely the
774 responsibility of the authors and does not necessarily represent the official views of the National Institutes
775 of Health, the March of Dimes, or the Burroughs Wellcome Fund.

776

777 **Author Contributions**

778 A.A., A.L.L., P.A., J.A.C, A.R. conceived and designed the study. A.A. and A.L.L performed all
779 statistical analyses, functional annotations, and wrote the manuscript under guidance from P.A., J.A.C,
780 A.R. G.Z. and L.M provided sPTB-associated genomic regions, guidance, and feedback on the
781 manuscript. Y.P. calculated the beta score measure for balancing selection using BetaScan³³. S.F.
782 calculated the alignment block age. All authors reviewed and approved the final manuscript.

783

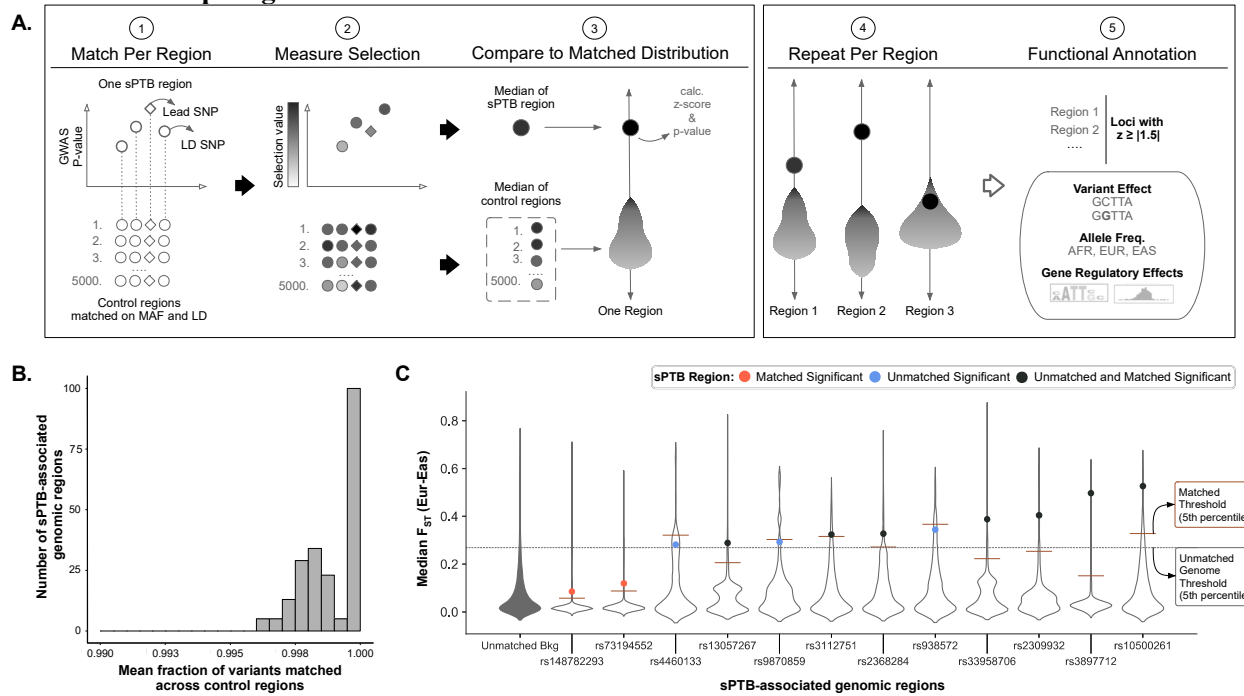
784 **Competing interests**

785 The authors declare no competing interests

786

787

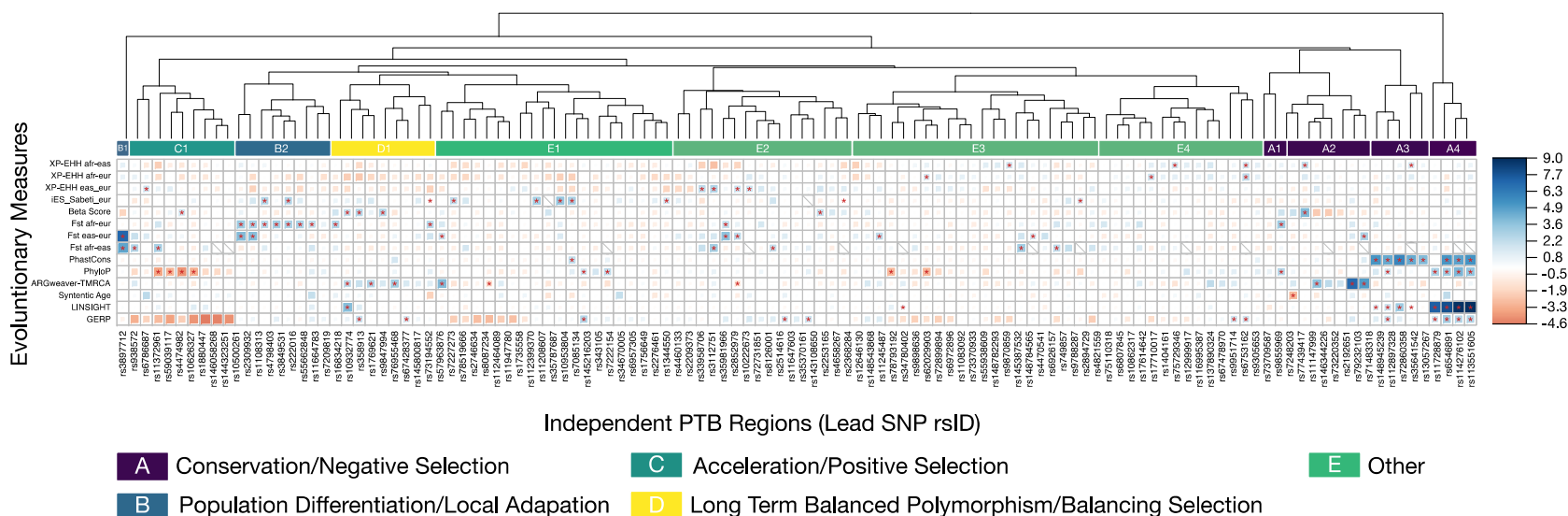
788 **Main Manuscript Figures**



789

790

791 **Figure 1: Accounting for minor allele frequency and linkage disequilibrium of sPTB-associated**
 792 **genomic regions identifies loci that have experienced diverse evolutionary forces.** **A.** We compared
 793 evolutionary measures for each sPTB-associated genomic region ($n=215$) to MAF and LD matched
 794 control regions (~ 5000). The sPTB-associated genomic regions each consisted of a lead variant ($p < 10E-4$
 795 association with sPTB) and variants in high LD ($r^2 > 0.9$) with the lead variant. Each control region has an
 796 equal number of variants as the corresponding sPTB-associated genomic region and is matched for MAF
 797 and LD ('Match Per Region'). We next obtained the values of an evolutionary measure for the variants
 798 included in the sPTB-associated regions and all control regions ('Measure Selection'). The median value
 799 of the evolutionary measure across variants in the sPTB-associated region and all control regions was
 800 used to derive a z-score ('Compare to Null Distributions'). We repeated these steps for each sPTB-
 801 associated region ('Repeat Per Region') and then functionally annotated sPTB-associated regions with
 802 absolute z-scores ≥ 1.5 ('Functional Annotation'). **B.** Across all sPTB-associated genomic regions, the
 803 mean fraction of variants matched across all control regions was ≥ 0.99 . **C.** A representative example for
 804 pairwise F_{ST} between East Asians (EAS) and Europeans (EUR). Violin plots display the unmatched
 805 genome background ('unmatched Bkg', dark fill) or the matched background (no fill) with the sPTB-
 806 region labeled by the lead variant (rsID), i.e. the variant with the lowest sPTB-association p-value. Each
 807 point represents the median value of F_{ST} for the sPTB-associated regions labeled by the lead SNP (rsID,
 808 x-axis). The dotted line represents the threshold for the top 5th percentile when randomly sampled
 809 ($n=5,000$) from the 'unmatched Bkg.' The solid horizontal line for each unfilled violin plot represents the
 810 5th percentile for matched background distribution. Each dot's color represents whether the region is
 811 significant by genome background (blue), matched background (red), or both (black). Note that
 812 significance is influenced by choice of background and that our approach identifies sPTB-associated
 813 regions that have experienced diverse evolutionary forces while controlling for important factors, such as
 814 MAF and LD.



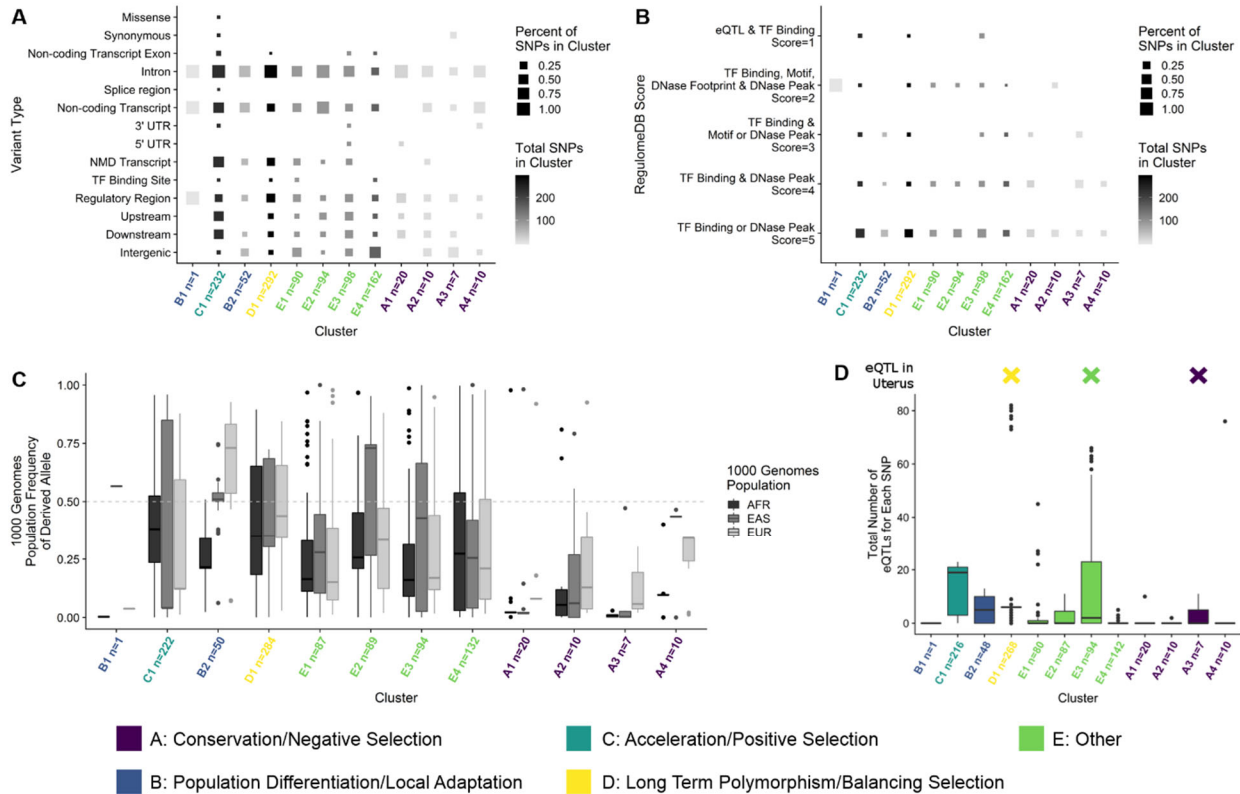
815

816

817 **Figure 2: Clusters of sPTB-associated genomic regions have experienced diverse evolutionary forces.** We tested sPTB-associated genomic
 818 regions (x-axis) for diverse types of selection (y-axis), including F_{ST} (population differentiation), XP-EHH (positive selection), Beta Score
 819 (balancing selection), allele age (time to most recent common ancestor, TMRCA, from ARGweaver), alignment block age, phyloP
 820 (positive/negative selection), GERP, LINSIGHT, and PhastCons (negative selection) (Table 1). The relative strength (size of square) and direction
 821 (color) of each evolutionary measure for each sPTB-associated region is presented as a z-score calculated from that region's matched background
 822 distribution. Only regions with $|z| \geq 1.5$ for at least one evolutionary measure before clustering are shown. Statistical significance was assessed by
 823 comparing the median value of the evolutionary measure to the matched background distribution to derive an empirical p-value ($*p > 0.05$).
 824 Hierarchical clustering of sPTB-associated genomic regions on their z-scores identifies distinct groups or clusters that appear to be driven by
 825 different types of evolutionary forces. Specifically, we interpret regions that exhibit higher than expected values for PhastCons, PhyloP,
 826 LINSIGHT, and GERP to have experienced conservation and negative selection (Group A); regions that exhibit higher than expected pairwise F_{ST}
 827 values to have experienced population differentiation/local adaptation (Group B); regions that exhibit lower than expected values for PhyloP to
 828 have experienced acceleration/positive selection (Group C); and regions that exhibit higher than expected Beta Score and older allele ages
 829 (TMRCA) to have experienced balancing selection (Group D). The remaining regions exhibit a variety of signatures that are not consistent with a
 830 single evolutionary mode (Group E).

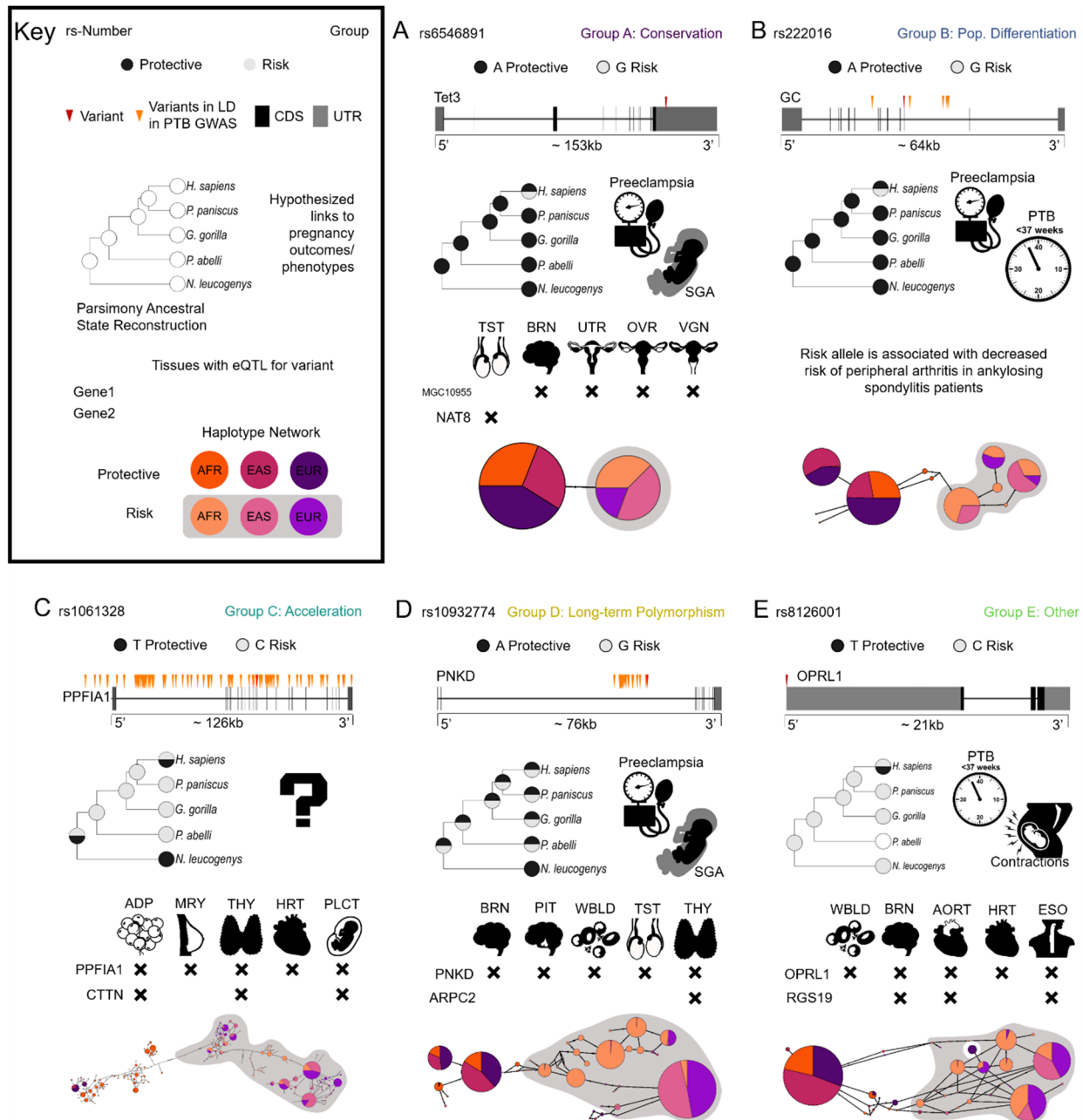
831

832



833

834 **Figure 3. Clusters of PTB regions that have experienced different types of selection vary widely in**
 835 **their molecular characteristics and functions.** Clusters are ordered as they appear in the z-score
 836 heatmap (Fig. 2) and colored by their major type of selection: Group A: Conservation and negative
 837 selection (Purple), Group B: Population differentiation/local adaptation (Blue), Group C: Acceleration
 838 and positive selection (Teal), Group D: Long term polymorphism/balancing selection (Teal), and Other
 839 (Green). **A.** The proportions of different types of variants (e.g., intronic, intergenic, etc.) within each
 840 cluster (x-axis) based on the Variant Effect Predictor (VEP) analysis. Furthermore, cluster C1 exhibits the
 841 widest variety of variant types and is the only cluster that contains missense variants. Most variants across
 842 most clusters are located in introns. **B.** The proportion of each RegulomeDB score (y-axis) within each
 843 cluster (x-axis). Most notably, PTB regions in three clusters (B1, A5, and D4) have variants that are likely
 844 to affect transcription factor binding and linked to expression of a gene target (Score=1). Almost all
 845 clusters contain some variants that are likely to affect transcription factor binding (Score=2). **C.** The
 846 derived allele frequency (y-axis) for all variants in each cluster (x-axis) for the African (AFR), East Asian
 847 (EAS), and European (EUR) populations. Population frequency of the derived allele varies within
 848 populations from 0 to fixation. **D.** The total number of eQTLs (y-axis) obtained from GTEx for all
 849 variants within each cluster (x-axis) All clusters but one (C2 with only one variant) have at least one
 850 variant that is associated with the expression of one or more genes in one or more tissues. Clusters A1,
 851 A5, and D4 also have one or more variants associated with expression in the uterus.



852
 853 **Figure 4: Functional and evolutionary characterizations of a representative variant from each**
 854 **group illustrate their diverse histories and roles in risk of preterm birth.** For each variant of interest,
 855 we report the following information listed from top to bottom: the protective and risk alleles as predicted
 856 by the sPTB GWAS¹³⁶; the location relative to the nearest gene of the variant and linked variants; the
 857 allelic data at this location across the great apes and the parsimony reconstruction of the ancestral allele(s)
 858 at this site; hypothesized links to pregnancy outcomes or phenotypes from previous studies; selected
 859 significant GTEx hits; and finally, the human haplotype(s) containing each variant in a haplotype map
 860 labeled by 1KG population. **A.** Representative variant from group A (conservation): rs6546894 contains a
 861 human-specific risk allele and is located in the 3' UTR of the gene *TET3*. The site has strong evidence of
 862 long-term evolutionary conservation. The gene *TET3* has been shown to be elevated in preeclamptic and
 863 small for gestational age (SGA) placentas⁵³. The rs6546894 variant is also associated with changes in

864 expression of genes *MGC10955* and *NAT8* in the testis (TST), brain (BRN), uterus (UTR), ovaries
865 (OVR), and vagina (VGN) tissues. The variant does not have high LD ($r^2 > 0.9$) with any other 1KG
866 variants so there are only two haplotypes/alleles. **B.** Representative variant from group B (population
867 differentiation): rs222016 is located in the intron of the gene *GC* and has a human-specific protective
868 allele. The gene *GC* is linked the occurrence of sPTB⁶⁵. This variant is not associated with any known
869 eQTLs, but the risk allele has been associated with a protective effect on arthritis⁵⁹. Haplotypes containing
870 the protective allele are rare in the African population. **C.** Representative variant from group C
871 (acceleration): rs1061328 is located in an intron of the gene *PPFIA1* and is in high LD with 156 other
872 variants spanning the gene's length. It has a protective allele that is human-specific. This variant is
873 associated with changes in expression of *PPFIA1* and *CTTN* genes in adipose cells (ADP), mammary
874 tissue (MRY), the thyroid (THY), and heart (HRT). The gene *CTTN* has been shown to be expressed in
875 placental cells^{85,86}. There is a total of 102 haplotypes associated with this variant. **D.** Representative
876 variant from group D (long-term polymorphism): rs10932774 is located in the intronic region of the gene
877 *PNKD* and is in high LD with 27 additional SNPs in an 8.8 kb region. Consistent with the action of
878 balancing selection, both alleles of the variant are found throughout the great apes. The gene *PNKD* is
879 upregulated in severely preeclamptic placentas⁹⁹ and *ARPC2* has been associated with SGA¹³⁷.
880 Expression changes associated with this variant include *PNKD* and *ARPC2* in the brain, pituitary gland
881 (PIT), whole blood (WBLD), testis, and thyroid (THY). Haplotypes containing the risk allele are more
882 prevalent across populations and also display greater haplotype diversity. **E.** Representative variant from
883 group E (other): rs8126001 is located in the 5' UTR of the gene *OPRL1* and has a human-specific
884 protective allele. The protein product of the *ORPL1* gene is the nociceptin receptor, which has been linked
885 to contractions and the presence of nociception in preterm uterus samples^{115,116}. This variant is associated
886 with expression of the genes *OPRL1* and *RGS19* in whole blood, the brain, aorta (AORT), heart, and
887 esophagus (ESO: eQTL data is from GTEx v6). There is more haplotype diversity in the risk allele and
888 these haplotypes are more prevalent in the European and African populations.

889

890